Biochemical Journal (2019) **476** 2939–2952
https://doi.org/10.1042/BCJ20190523

PORTLAND PRESS

Research Article

Biochemical characterization of phospho*enol*pyruvate carboxykinases from *Arabidopsis thaliana*

Bruno E. Rojas[1], Matías D. Hartman[1,*], Carlos M. Figueroa[1], Laura Leaden[2,†], Florencio E. Podestá[2] and Alberto A. Iglesias[1]

[1]Instituto de Agrobiotecnología del Litoral, UNL, CONICET, FBCB, Santa Fe, Argentina; [2]Centro de Estudios Fotosintéticos y Bioquímicos, UNR, CONICET, FCByF, Rosario, Argentina

Correspondence: Alberto A. Iglesias (iglesias@fbcb.unl.edu.ar)

ATP-dependent phospho*enol*pyruvate carboxykinases (PEPCKs, EC 4.1.1.49) from C_4 and CAM plants have been widely studied due to their crucial role in photosynthetic CO_2 fixation. However, our knowledge on the structural, kinetic and regulatory properties of the enzymes from C_3 species is still limited. In this work, we report the recombinant production and biochemical characterization of two PEPCKs identified in *Arabidopsis thaliana*: *Ath*PEPCK1 and *Ath*PEPCK2. We found that both enzymes exhibited high affinity for oxaloacetate and ATP, reinforcing their role as decarboxylases. We employed a high-throughput screening for putative allosteric regulators using differential scanning fluorometry and confirmed their effect on enzyme activity by performing enzyme kinetics. *Ath*PEPCK1 and *Ath*PEPCK2 are allosterically modulated by key intermediates of plant metabolism, namely succinate, fumarate, citrate and α-ketoglutarate. Interestingly, malate activated and glucose 6-phosphate inhibited *Ath*PEPCK1 but had no effect on *Ath*PEPCK2. Overall, our results demonstrate that the enzymes involved in the critical metabolic node constituted by phospho*enol*pyruvate are targets of fine allosteric regulation.

Introduction

Phospho*enol*pyruvate (PEP) is a key metabolic intermediate because it is a high-energy compound ($\Delta G = -14.8$ kcal mol^{-1} for PEP hydrolysis) and it participates in many enzymatic reactions [1]. PEP is also important to connect a variety of metabolic pathways, including glycolysis, gluconeogenesis and organic acid metabolism [1,2]. Among the many enzymes that metabolize PEP, PEP carboxykinase (PEPCK) is particularly relevant. Based on the phosphate donor employed, PEPCKs can be classified as ATP- (EC 4.1.1.49), GTP- (EC 4.1.1.32) or PPi-dependent (EC 4.1.1.38), with different evolutionary origins [2–5]. The ATP-dependent PEPCK is present in bacteria, yeasts and plants. This enzyme reversibly catalyzes oxaloacetate (OAA) decarboxylation, according to the reaction: OAA + ATP ↔ PEP + ADP + CO_2. PEPCK has an absolute requirement of divalent cations for its activity [6]. One metal ion acts as an essential activating cofactor, with Mn^{2+} the most activating [5–8]. A second divalent cation (either Mn^{2+} or Mg^{2+}) is involved in forming the metal–nucleotide complex that constitutes the active form of the substrate [6].

In plants, PEPCK is well known for its central role in the CO_2 concentrating mechanisms operating in C_4 [9,10] and CAM photosynthesis [11], where it provides CO_2 to the Benson–Calvin cycle by decarboxylating the OAA derived from malate or aspartate. Also, PEPCK has a crucial role during seed germination, channeling carbon released from fatty acid reserves to form sugars until the development of the photosynthetic apparatus [12–16]. It has also been suggested that this enzyme is involved in nitrogen and amino acid metabolism [17,18]. *Arabidopsis thaliana* has two putative *PEPCK* genes (AT4G37870 and AT5G65690, coding for *Ath*PEPCK1 and *Ath*PEPCK2, respectively),

*Current address: Max Planck Institute for Biology of Ageing, Cologne, Germany.
†Current address: Departamento de Microbiologia, Instituto de Ciências Biomédicas, Universidade de São Paulo, São Paulo, Brazil.

Received: 12 July 2019
Revised: 19 September 2019
Accepted: 23 September 2019

Accepted Manuscript online: 23 September 2019
Version of Record published: 18 October 2019

PORTLAND PRESS

Biochemical Journal (2019) 476 2939–2952
https://doi.org/10.1042/BCJ20190523

which are expressed in most plant tissues [19]. The key role of PEPCK in gluconeogenesis has been clearly established in germinating seeds of this species using various experimental approaches [20–23]. However, the biochemical and regulatory properties of both isozymes remain largely unknown.

In this work, we cloned the genes coding for *Ath*PEPCK1 and *Ath*PEPCK2 and expressed them in *Escherichia coli*. The recombinant enzymes thus produced were highly purified and characterized. Our results show that both enzymes are more efficient to catalyze the decarboxylation of OAA *in vitro*. We also identified metabolites that differentially affect the activity of *Ath*PEPCK1 and *Ath*PEPCK2, which could modulate both isozymes under differential physiological conditions. Our results aim to bring new insights into the biochemical regulation of PEPCKs of C_3 species and to integrate these findings with the metabolic and developmental data available in the literature, to better understand the regulation of PEP metabolism in C_3 plants.

Experimental

Reagents

ATP, ADP, PEP, OAA, NADH, Glc6P, L-malic acid, pyruvate kinase (PK) and malic dehydrogenase were purchased from Sigma–Aldrich. L-lactate dehydrogenase was purchased from Roche. All other reagents were of the highest available quality.

Cloning, expression and purification of *Ath*PEPCKs

Sequences coding for *Ath*PEPCK1 (AT4G37870) and *Ath*PEPCK2 (AT5G65690) were retrieved from the TAIR database [24]. The gene coding for *Ath*PEPCK1 was amplified from the pCMV-Sport6/PEPCK vector (kindly provided by Dr. C. Lacomme from INRA, CNRGV Plant Genomic Center, Toulouse, France). The sequence coding for *Ath*PEPCK2 was *de novo* synthesized using optimized codons for expression in *E. coli* (Bio Basic). Both genes were cloned between *Sac*I and *Sal*I sites within the multiple cloning site 1 of the pRSFDuet-1 vector (Novagen), in frame with an N-terminal His_6-tag.

*Ath*PEPCK1 was expressed in *E. coli* SHuffle T7 (New England BioLabs), while *Ath*PEPCK2 was expressed in *E. coli* BL21 (DE3) (Invitrogen). Cells were grown in LB medium supplemented with 50 μg ml^{-1} kanamycin (and 100 μg ml^{-1} spectinomycin in the case of SHuffle T7 cells) and protein expression was induced with 0.5 mM isopropyl-β-D-1-thiogalactopyranoside for 16 h at 25°C and 180 rpm. Cells were harvested by centrifugation, resuspended in lysis buffer [25 mM Tris–HCl pH 8.0, 300 mM NaCl, 5% (v/v) glycerol and 10 mM imidazole], disrupted by sonication and centrifuged twice at 12 000×***g*** for 20 min at 4°C. The crude extract was loaded onto a 1-ml HisTrap HP column previously equilibrated with lysis buffer, connected to an ÄKTA Explorer 100 system (GE Healthcare). Proteins were eluted with a linear imidazole gradient (10–300 mM) in lysis buffer. Fractions containing PEPCK activity were pooled, concentrated and stored at −80°C until use. Under these conditions, both enzymes remained fully active for at least three months.

Native molecular mass determination

Protein molecular mass was determined by gel filtration chromatography using a Superdex 200 10/300 column (GE Healthcare) equilibrated with 50 mM HEPES pH 8.0 and 100 mM NaCl. A calibration curve was constructed by plotting K_{av} values versus log(molecular mass) of protein standards, including thyroglobulin (669 kDa), ferritin (440 kDa), aldolase (158 kDa), conalbumin (75 kDa), ovalbumin (44 kDa), carbonic anhydrase (29 kDa) and ribonuclease (13.7 kDa). K_{av} values were calculated as $(V_e - V_0)/(V_t - V_0)$, where V_e is the elution volume of the protein, V_0 is the elution volume of Dextran Blue (Promega) and V_t is the total volume of the column.

Enzyme activity assays

The standard conditions for PEPCK activity measurements consisted of 100 mM HEPES–NaOH pH 7.0, 4 mM β-mercaptoethanol, 4 mM $MgCl_2$, 10 μM $MnCl_2$ and 0.2 mM NADH. The reaction in the direction of PEP carboxylation contained (unless otherwise specified): 90 mM $KHCO_3$, 2 U malate dehydrogenase, 0.13 mM ADP and 10 mM PEP. The reaction in the direction of OAA decarboxylation contained (unless otherwise specified): 1 U PK, 1 U lactate dehydrogenase, 0.75 mM ATP and 0.75 mM OAA (freshly prepared). Assays were performed in 50 μl at 30°C.

Kinetic parameters were calculated using the software OriginPro 8 (OriginLab Corporation). Activity data were plotted against the concentration of the variable substrate or effector and fitted to a modified Hill

Biochemical Journal (2019) **476** 2939–2952
https://doi.org/10.1042/BCJ20190523

equation: $v = v_0 + (V - v_0) \times C^{nH}/(k^{nH} + C^{nH})$; where v is the initial velocity; v_0 is the velocity in absence of the substrate or effector being analyzed; V is the maximal velocity (V_{max}), activation or inhibition; C is the concentration of substrate or effector under study; k is the concentration of substrate or effector producing half of the maximal velocity (K_m), activation ($A_{0.5}$) or inhibition ($I_{0.5}$); and n_H is the Hill coefficient. Substrate kinetic parameters were calculated fixing the n_H to 1, which turns the modified Hill equation into the classical Michaelis–Menten equation. One unit (U) is defined as the amount of enzyme that catalyzes the formation of 1 μmol of the product (PEP or OAA) per minute under the specified assay conditions (of decarboxylation or carboxylation, respectively). Allosteric effectors were assayed under standard conditions (see above). Before performing these experiments, effectors were tested on coupled enzymes to avoid unwanted effects.

Protein thermal shift assays

To analyze metabolite binding to the recombinant enzymes, we employed thermal shift assays coupled to differential scanning fluorometry according to the method described by Ericsson et al. [25]. Assays were performed in a final volume of 20 μl with 0.15 mg ml^{-1} protein, 4X Sypro Orange (Sigma) and 25 mM HEPES–NaOH pH 7.0 in MicroAmp fast 96-well PCR plates (Applied Biosystems). All the reactions were performed with their corresponding controls (without protein or effector). Plates were sealed with Microseal adhesive film (Bio-Rad) and heated in a StepOne Real-Time PCR System (Applied Biosystems) from 25 to 99°C, with increments of 0.4°C. Changes in fluorescence were monitored simultaneously. The wavelengths for excitation and emission were 490 and 575 nm, respectively. Melting temperature (T_m) of each sample was calculated by plotting the first derivative of the fluorescence emission ($-dF/dT$) as a function of temperature (T) and identifying the minimum of the curve. The shift in the melting temperature (ΔT_m) was calculated subtracting each T_m to the control without effector.

Results

Arabidopsis genome contains two genes coding for putative PEPCKs [24]. The *AT4G37870* gene encodes a putative protein (*Ath*PEPCK1) of 672 amino acids with theoretical pI of 6.63 and estimated mass of 73.5 kDa, while the *AT5G65690* gene codes for a putative protein (*Ath*PEPCK2) of 671 amino acids with theoretical pI of 5.99 and estimated mass of 73.0 kDa. The sequence identity between both proteins is 78.4% (86.5% similarity), being the main differences found at the first 150 amino acids (Supplementary Figure S1). We cloned the sequences coding for *Ath*PEPCK1 and *Ath*PEPCK2 and the recombinant proteins were expressed with a 2 kDa tag (including the His_6-tag) at the N-termini. These enzymes were purified by immobilized nickel affinity chromatography (IMAC-Ni^{2+}), yielding highly pure (>90%) protein preparations, with molecular masses of ~75 kDa (Figure 1A). The purified recombinant enzymes exhibited specific activity values of 3 and 5 U mg^{-1}

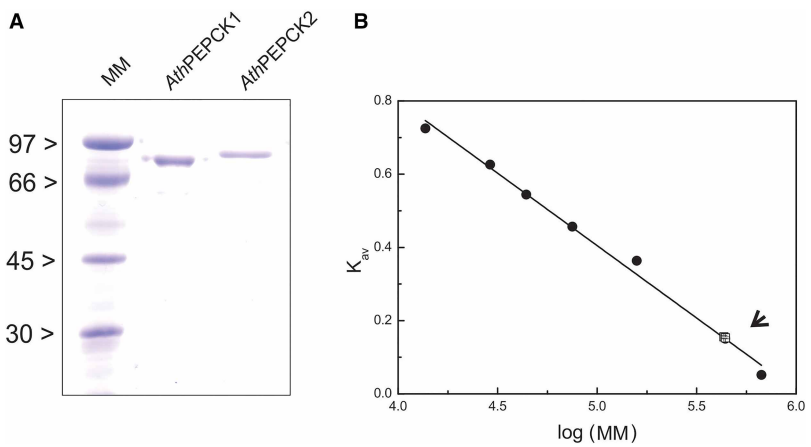

Figure 1. Purification and native molecular mass determination for *Ath*PEPCK1 and *Ath*PEPCK2.

(**A**) The purified *Ath*PEPCK1 and *Ath*PEPCK2 were analyzed by 12% SDS–PAGE; MM: molecular mass marker. (**B**) Superdex 200 gel filtration calibration curve constructed using the protein standards described in the Experimental section. For the samples (indicated with an arrow), the data shown are the mean of two experiments.

Biochemical Journal (2019) **476** 2939–2952
https://doi.org/10.1042/BCJ20190523

(*Ath*PEPCK1 and *Ath*PEPCK2, respectively), when assayed in the direction of OAA decarboxylation under the standard condition described in the Experimental section. Based on their migration in the gel filtration column (Figure 1B and Supplementary Figure S2), we determined that both enzymes are hexamers of ∼440 kDa. The activity of *Ath*PEPCKs was maximal at pH 7.0 with HEPES–NaOH in both directions of the reaction (Supplementary Figure S3), a similar behavior to that observed for other plant PEPCKs [8,26–29]. We chose this buffer to perform the kinetic characterization of both enzymes because its interaction with metal ions is negligible [30] and the pH value is very close to that found in the plant cytosol (7.3 ± 0.1) [31–33].

PEPCK activity is dependent on both Mg^{2+} and Mn^{2+} ions; the former is necessary to form the true substrate (ATP–Mg^{2+}) and the latter acts as an activator [8]. We analyzed the effect of increasing Mn^{2+} concentration at a fixed Mg^{2+} level, and *vice versa*, on *Ath*PEPCK1 and *Ath*PEPCK2. These experiments were done in the carboxylation direction because measuring PEPCK activity on the opposite direction requires the obligate addition of a metal ion for PK [34]. The highest activity values (∼3.5 U mg^{-1} for *Ath*PEPCK1 and ∼6.0 U mg^{-1} for *Ath*PEPCK2) were obtained at 1 mM Mn^{2+} in absence of Mg^{2+}, whereas the presence of 0.5 mM Mg^{2+} decreased ∼2-fold the activity of both enzymes (Figure 2A,C). The opposite pattern was observed at low Mn^{2+} concentrations (0 to 0.1 mM), since the presence of 0.5 mM Mg^{2+} slightly increased their activity (Figure 2A,C). *Ath*PEPCK1 and 2 scarcely responded to Mg^{2+} in the absence of Mn^{2+}; however, a concentration as low as 10 μM Mn^{2+} produced a discrete response to Mg^{2+} (Figure 2B,D). Within plant cells, cytosolic Mn^{2+} concentration has been reported to be in the 0.3–0.8 μM range [35,36]; therefore, kinetic parameters

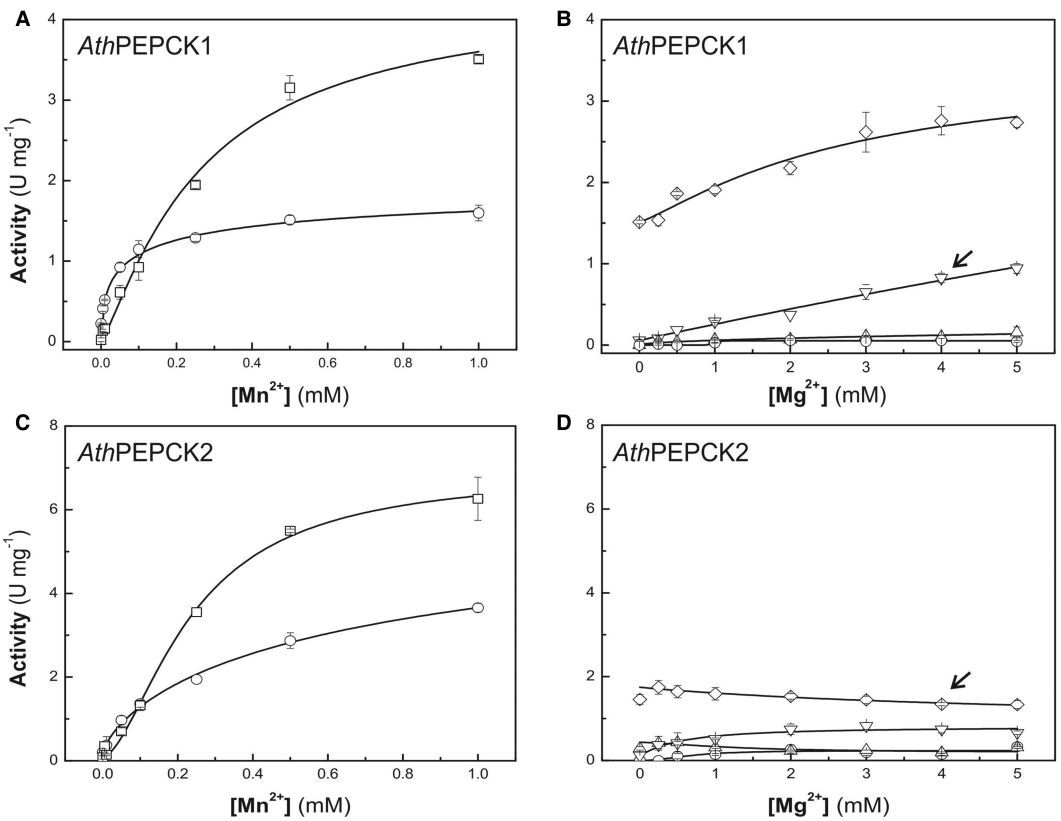

Figure 2. Metal ion dependence of AthPEPCKs carboxylation activity.

*Ath*PEPCK1 (**A**) and *Ath*PEPCK2 (**C**) activity was measured at increasing Mn^{2+} concentration in absence (squares) or presence of 0.5 mM Mg^{2+} (circles). *Ath*PEPCK1 (**B**) and *Ath*PEPCK2 (**D**) activity was measured at increasing Mg^{2+} concentration in the absence (up triangles) or presence of 10 μM (inverted triangles) or 100 μM of Mn^{2+} (diamonds). A control with 0.1 mM of EGTA was added to eliminate traces of Mn^{2+} (circles). Substrate concentrations were 0.3 mM ADP and 6 mM PEP. The arrows indicate the physiological concentration of metals chosen for further kinetic characterization. Data are the mean of two independent data sets ± SE.

were determined at physiological concentrations of both metal ions (4 mM Mg^{2+} and 10 μM Mn^{2+}), as previously reported by Chen et al. [37].

Substrate kinetics for *Ath*PEPCK1 and 2 were performed in both directions of catalysis (Table 1 and Supplementary Figures S4 and S5). Both enzymes exhibited affinity (estimated from K_m values) of more than one order of magnitude higher for the binding of OAA compared with PEP. In the case of the nucleotides, ADP and ATP affinities were in the same range. In general, the specific activity and substrate affinities were higher for *Ath*PEPCK2 than *Ath*PEPCK1 (Table 1). Values of V_{max} in the decarboxylation direction were slightly higher (up to 2-fold) compared with those observed for the carboxylation reaction. These results support that *Ath*PEPCKs preferentially catalyze the decarboxylation of OAA than the carboxylation of PEP (see catalytic efficiencies reported in Table 1).

Enzymes involved in key metabolic steps are generally regulated by different mechanisms. From these, allosteric regulation plays a critical role on the fine control of enzymatic activities [38–41]. To identify putative modulators of *Ath*PEPCKs activity we performed thermal shift assays [42–45], using a broad range of metabolites from several metabolic pathways that could potentially act as enzyme ligands. In our experiments, melting curves were highly reproducible (an example is shown in Supplementary Figure S6), with coefficients of variation lower than 1.5%. Among the tested metabolites, those that significantly modified the T_m of *Ath*PEPCKs were: fructose 6-phosphate (Fru6P), glucose 6-phosphate (Glc6P), glucose 1-phosphate (Glc1P), fructose 1,6-bisphosphate (Fru1,6bisP), 3-phosphoglycerate (3PGA), inorganic pyrophosphate (PPi), the PEP-analogue *N*-(phosphonomethyl)glycine, pyruvate (Pyr), acetyl-CoA, citrate, malate, succinate, fumarate, L-glutamate (L-Glu), shikimate, L-arginine (L-Arg) and L-aspartate (L-Asp). Interestingly, the T_m increase for some metabolites was dependent on their concentration (Figure 3).

Afterwards, we assessed the effect of the putative regulators on the decarboxylation activity of each enzyme (Figure 4 and Supplementary Figure S7). Glc6P, Fru6P and Glc1P inhibited *Ath*PEPCK1 but not *Ath*PEPCK2, whereas Fru1,6bisP inhibited both enzymes. In the case of *Ath*PEPCK1, Glc6P produced the strongest inhibition (~75%) at the highest concentration tested, whereas Glc1P, Fru6P and Fru1,6bisP produced ~50% inhibition at the same concentration (Figure 4 and Supplementary Figure S7). For *Ath*PEPCK1, the $I_{0.5}$ values for Glc6P and Fru1,6bisP were 8.1 and 16 mM, respectively, whereas Glc1P and Fru6P exhibited $I_{0.5}$ values ~3-fold higher than Glc6P (Table 2).

The organic acids anions α-ketoglutarate, fumarate, succinate and citrate displayed similar inhibition patterns for both enzymes, with fumarate showing the lowest $I_{0.5}$ value (Table 2 and Supplementary Figure S7). To test whether the observed inhibition was due to free metal sequestration, we performed the same curves but preparing the organic acids with an equimolecular amount of Mg^{2+}. Under the new conditions, the $I_{0.5}$ values of *Ath*PEPCK1 for α-ketoglutarate, fumarate and succinate were similar to those observed before adding Mg^{2+} (Table 2). Instead, the effect of these molecules on *Ath*PEPCK2 became negligible, suggesting that inhibition

Table 1 Substrate kinetic parameters for AthPEPCK1 and AthPEPCK2

Enzyme	Reaction direction	Substrate	K_m (μM)	V_{max} (U mg^{-1})	Catalytic efficiency (× 10^3 M^{-1} s^{-1})
*Ath*PEPCK1	Carboxylation	PEP[a]	3700 ± 500	1.40 ± 0.03	0.5 ± 0.1
		ADP[b]	79 ± 1		25 ± 2
	Decarboxylation	OAA[c]	230 ± 20	2.6 ± 0.3	13 ± 3
		ATP[d]	72 ± 2		39 ± 5
*Ath*PEPCK2	Carboxylation	PEP[a]	3800 ± 300	3.2 ± 0.1	1.1 ± 0.1
		ADP[b]	39 ± 4		100 ± 16
	Decarboxylation	OAA[c]	100 ± 10	5.4 ± 0.1	82 ± 6
		ATP[d]	18 ± 3		370 ± 42

Reactions were performed as described in the Experimental section. Constants were calculated by fitting experimental data to the modified Hill equation fixing n_H to 1 (Supplementary Figures S4 and S5). Reported values are the mean ± SE obtained from the fitting software. Fixed substrate concentrations used were as follows:
[a]0.25 mM ADP;
[b]15 mM PEP;
[c]0.75 mM ATP;
[d]0.75 mM OAA.

Biochemical Journal (2019) **476** 2939–2952
https://doi.org/10.1042/BCJ20190523

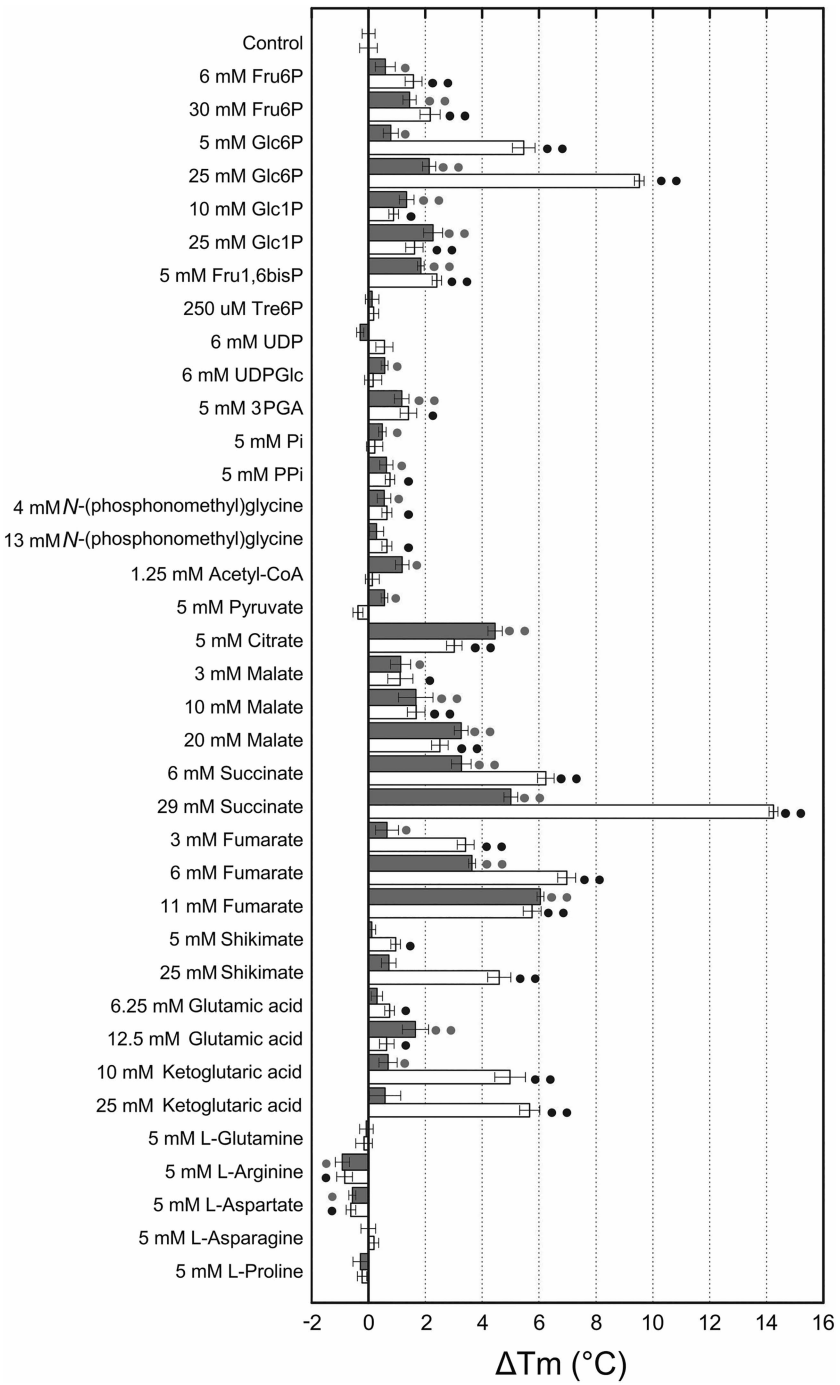

Figure 3. High-throughput screening of effectors binding to *Ath*PEPCK1 (grey bars) and *Ath*PEPCK2 (white bars) by thermal shift assays coupled to differential scanning fluorometry.

Experiments were performed in the presence of different concentrations of effectors (as indicated in the figure) and the shift in the melting temperature was calculated as described in the Experimental section. Data are the mean ± SE of three replicates for all samples and nine replicates for the control without ligand. • indicates a P-value < 0.05 and •• indicates a P-value < 0.01 using a t-test for two independent samples with a confidence level of 95%.

Biochemical Journal (2019) **476** 2939–2952
https://doi.org/10.1042/BCJ20190523

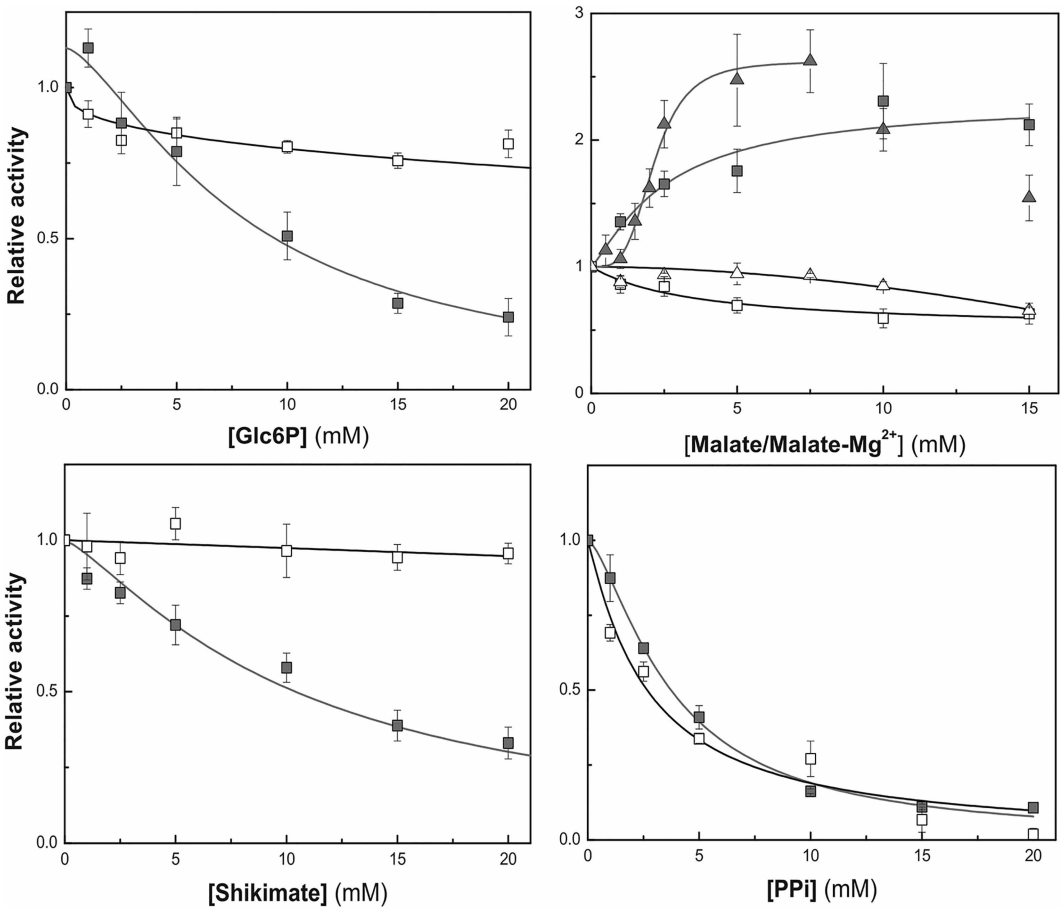

Figure 4. Allosteric modulators of *Ath*PEPCKs.

The activity of *Ath*PEPCK1 (grey squares) and *Ath*PEPCK2 (white squares) was measured at increasing concentrations of the metabolites indicated in the figure. Measurements were done as described in the Experimental section, in presence of 0.75 mM ATP and 0.75 mM OAA. The effect of malate was studied in the carboxylation direction at fixed substrate concentrations (0.13 mM ADP and 10 mM PEP) and variable concentrations of malate (squares) or malate-Mg^{2+} (triangles). Data are the mean of four independent data sets ± SE. Data were adjusted to a modified Hill equation (calculated parameters are shown in Table 2).

was caused by free metal depletion. Similarly, further addition of Mg^{2+} reduced the inhibition caused by citrate, reflected by the increase in the $I_{0.5}$ values (Table 2 and Supplementary Figure S7). Interestingly, malate activated *Ath*PEPCK1 but had no effect on *Ath*PEPCK2, while the presence of an equimolecular concentration of Mg^{2+} slightly increased the response of *Ath*PEPCK1 to the activator (Figure 4 and Table 2). Shikimate and L-Glu also inhibited *Ath*PEPCK1 but not *Ath*PEPCK2 (Figure 4, Supplementary Figure S7 and Table 2). Considering all the effectors tested, PPi exerted the highest degree of inhibition (90%) and displayed the lowest $I_{0.5}$ value (3.7 and 2.7 mM for *Ath*PEPCK1 and *Ath*PEPCK2, respectively; Figure 4 and Table 2). To rule out the possibility that PPi inhibition was caused by free metal sequestration, we performed PPi curves with equimolecular concentrations of Mg^{2+}; under these conditions, the results were similar to those obtained without further additions of the divalent cation (data not shown).

Discussion

The properties of PEPCKs from photosynthetic organisms have been poorly explored in comparison with their counterparts from other organisms, with only a few reports on the literature (Supplementary Table S1). To expand our knowledge on the role of this enzyme in plant metabolism, we performed a detailed

Biochemical Journal (2019) **476** 2939–2952
https://doi.org/10.1042/BCJ20190523

Table 2 Kinetic parameters for allosteric effectors of AthPEPCKs

	***Ath*PEPCK1**		***Ath*PEPCK2**	
Effector	**$I_{0.5}$ (mM)**	**n_H**	**$I_{0.5}$ (mM)**	**n_H**
Glc6P	8.1 ± 0.8	1.5 ± 0.2	N.E.[b]	—
Glc1P	26 ± 2	1.5 ± 0.2	N.E.	—
Fru6P	27 ± 2	0.9 ± 0.1	N.E.	—
Fru1,6bisP	16 ± 1	1.2 ± 0.1	43 ± 5	0.8 ± 0.1
3PGA	21 ± 2	1.5 ± 0.2	35 ± 3	0.9 ± 0.1
PPi	3.7 ± 0.1	1.5 ± 0.1	2.7 ± 0.4	1.1 ± 0.2
Pyruvate[a]	15 ± 2	1.1 ± 0.2	27 ± 3	2.9 ± 0.8
N-(phosphonomethyl)glycine	6.1 ± 0.6	0.8 ± 0.1	21 ± 4	0.9 ± 0.1
α-ketoglutarate	13 ± 1	1.7 ± 0.4	41 ± 12	0.4 ± 0.1
α-ketoglutarate-Mg^{2+}	19 ± 2	1.1 ± 0.1	N.E.	—
Fumarate	8.6 ± 0.5	1.7 ± 0.2	10 ± 1	1.8 ± 0.4
Fumarate-Mg^{2+}	9.6 ± 0.7	1.9 ± 0.3	N.E.	—
Succinate	12.1 ± 0.4	1.4 ± 0.1	11 ± 1	0.9 ± 0.1
Succinate-Mg^{2+}	14.5 ± 0.6	3.5 ± 0.6	18 ± 1	3.7 ± 0.9
Citrate	2.1 ± 0.1	1.4 ± 0.1	3.7 ± 0.7	1.4 ± 0.4
Citrate-Mg^{2+}	10.3 ± 0.6	1.5 ± 0.2	11.0 ± 0.6	2.3 ± 0.3
Shikimate	10.4 ± 0.9	1.3 ± 0.1	N.E.	—
L-Glu	32 ± 5	0.9 ± 0.1	N.E.	—
UDP	N.E.	—	8 ± 1	0.8 ± 0.1
	***Ath*PEPCK1**		***Ath*PEPCK2**	
	$A_{0.5}$ (mM)	**n_H**	**$A_{0.5}$ (mM)**	**n_H**
Malate[a]	2.6 ± 0.5	1.2 ± 0.3	N.E.	—
Malate-Mg^{2+}[a]	2.1 ± 0.1	4.1 ± 0.8	N.E.	—

Reactions were done as described in the Experimental section with fixed substrate concentrations of 0.75 mM ATP and 0.75 mM OAA. Constants were calculated by fitting experimental data presented in Figure 4 and Supplementary Figure S7 to the modified Hill equation.
[a]To test the effect of malate and pyruvate, activity was measured in the carboxylation direction with substrate concentrations of 0.13 mM ADP and 10 mM PEP.
[b]No effect was observed.

characterization of the kinetic and regulatory properties of the two PEPCKs present in Arabidopsis. One major hindrance for the study of source-derived PEPCK from C_3, C_4 and CAM species is its extreme sensitivity to proteolysis and multiple phosphorylation [11,14,46]. For these reasons, the use of recombinant enzymes is a convenient strategy to obtain homogeneous non-phosphorylated, non-proteolyzed enzyme preparations suitable for biochemical characterization [47,48]. This protocol should eliminate the discrepancies in the reported kinetic parameters (for example ∼6-fold differences in the K_m for OAA in the case of *Panicum maximum*) due to different populations of the enzymes purified from a plant source [8,11,12,27,28,37,49].

We determined that recombinant *Ath*PEPCKs are hexamers (Figure 1 and Supplementary Figure S2), the same quaternary structure reported for enzymes from C_4 species (*Urochloa panicoides*, *Chloris gayana* and *Panicum maximum*) [8], but different from those reported for PEPCK from *Cucurbita pepo* [29,50] and a small version of the protein present in *Anana comosus* [11]. The hexameric structure has been recently confirmed *in vivo* in a paper published by Veyel et al. [41]. These authors reported that *Ath*PEPCK1 possesses a native mass of 447 kDa in *A. thaliana* crude extracts, when analyzed by size exclusion chromatography coupled to protein identification by mass spectrometry (Supplementary material of reference [41]).

Traditionally, PEPCK activity was assayed with relatively high concentrations of Mn^{2+} (0.5–5 mM), conditions where the maximal activity is obtained (Figure 2A,C and Supplementary Table S1). However, as the concentration of this metal in plants cells remains within the micromolar range [35,37], in this work we characterized the recombinant enzymes from Arabidopsis using a physiological concentration of Mn^{2+} [37], to provide physiologically meaningful conclusions. Substrate kinetics determined under physiological conditions (4 mM $MgCl_2$ plus 10 μM $MnCl_2$) for *Ath*PEPCKs are in good agreement with those reported for enzymes from other plant species (Table 1 and Supplementary Table S1). Considering that the reaction catalyzed by PEPCK is fully reversible *in vitro*, the higher apparent affinity for OAA and ATP exhibited by both recombinant enzymes (Table 1) is in accordance with the view that they primarily operate in the decarboxylation direction (gluconeogenic pathway) *in vivo*. Nevertheless, there might be circumstances when the carboxylation reaction is stimulated, as it has been recently described for an acetylated mammalian GTP-dependent PEPCK [51]. Strikingly, PEPCKs from C_3 plants are relatively less active than the ones from C_4 and CAM species (Table 1 and Supplementary Table S1). The activities of *Ath*PEPCKs are similar to that from *C. pepo*, a C_3 species (Supplementary Table S1). Conversely, PEPCKs from species performing C_4 photosynthesis show ∼10-fold higher activity than *Ath*PEPCKs (Supplementary Table S1). We speculate this is due to the key role that PEPCKs play in the CO_2 concentrating mechanism operating in C_4 species.

To test the ability of recombinant *Ath*PEPCKs to bind putative effectors, we employed thermal shift assays coupled to differential scanning fluorometry. This technique was developed for high-throughput screening of ligands that might affect protein activity [52], becoming a fast, robust and economical technique to screen for enzyme effectors [42–45]. The changes obtained in the T_m can be compared with those obtained by isothermal calorimetry and with IC_{50} values from enzymatic assays [42]. Using this method, several metabolites were identified as potential *Ath*PEPCKs effectors. It is important to note that there was not a direct relationship between the increase in the melting temperature and the effect exerted by the ligand. For example, PPi was the most potent inhibitor of both *Ath*PEPCKs, but it only increased the T_m of *Ath*PEPCK1 and *Ath*PEPCK2 by 0.7 and 0.8°C, respectively (Figures 3 and 4). Conversely, succinate displayed the highest T_m increase (5°C for *Ath*PEPCK1 and 14°C for *Ath*PEPCK2), but it only mediated a mild inhibition (Figure 3 and Supplementary Figure S6).

PEPCKs from the C_4 plants *U. panicoides* and *C. gayana* are inhibited by 3PGA, Fru6P and Fru1,6bisP [8], as we observed for *Ath*PEPCK1 (Table 2). On the other hand, the enzymes from these C_4 plants were insensitive to L-Glu and malate, an inhibitor and an activator of *Ath*PEPCK1, respectively [8,53]. In the case of the enzyme from *C. pepo* (a C_3 plant), no effect was observed with succinate, malate and Fru1,6bisP [12], but this might be due to degradation of the enzyme as a consequence of the conditions employed in the purification [50]. A short version of a PEPCK present in the CAM plant *A. comosus* [11] is also inhibited by 3PGA and Fru1,6bisP, but succinate activated the pineapple enzyme while it inhibited *Ath*PEPCKs. Also, malate had no effect on the enzyme of *A. comosus* although it activated *Ath*PEPCK1 (Table 2).

PEP is involved in a complex metabolic network with multiple feedback controls [1]. It has been proposed that PEPCK activity is crucial during germination of oilseeds [20–23,54]. Mutation of the *PEPCK1* gene impairs the establishment of Arabidopsis seedlings [21,22]. We estimated that the cytosolic concentration of malate in Arabidopsis seedlings is close to 11 mM [55,56], a value considerably higher than the $A_{0.5}$ of malate determined for *Ath*PEPCK1 (Table 2). With this scenario in mind, we propose that activation of *Ath*PEPCK1 by malate might be a mechanism to stimulate the flux of carbon released from fatty acids degradation through the glyoxylate cycle into gluconeogenesis (Figure 5A). This would allow the synthesis of sugars to feed the seedling until the development of the photosynthetic apparatus is complete.

Enzymes that catalyze opposite reactions and function in the same subcellular compartment are often regulated in a reciprocal way to avoid futile cycles [1,57]. Such cycle would occur by simultaneous operation of PEPCK and phospho*enol*pyruvate carboxylase (PEPC, EC 4.1.1.31) which, if not regulated, would cause the net hydrolysis of ATP to ADP and Pi. Malate activates *Ath*PEPCK1 in the direction of PEP synthesis (Table 2) and, at the same time, it inhibits PEPC, which uses PEP [58–64], providing the necessary regulation (Figure 5A). As previously mentioned, plant PEPCKs are phosphorylated [29,46,65–69]. Leegood and Walker [67] proposed that this mechanism might coordinate the activities of both enzymes. In leaves of C_4 and CAM plants, light promotes the dephosphorylation of PEPC (reducing its activity and making it less sensitive to activators and more sensitive to inhibitors) and PEPCK (which increases its activity). Mass spectrometry data available in the PhosPhat database [70] show that both *Ath*PEPCK1 and *Ath*PEPCK2 are subject to phosphorylation on multiple sites (Supplementary Figure S1). Nevertheless, the effects on kinetic parameters or the tissues and physiological conditions where phosphorylation occurs remain to be elucidated.

Biochemical Journal (2019) 476 2939–2952
https://doi.org/10.1042/BCJ20190523

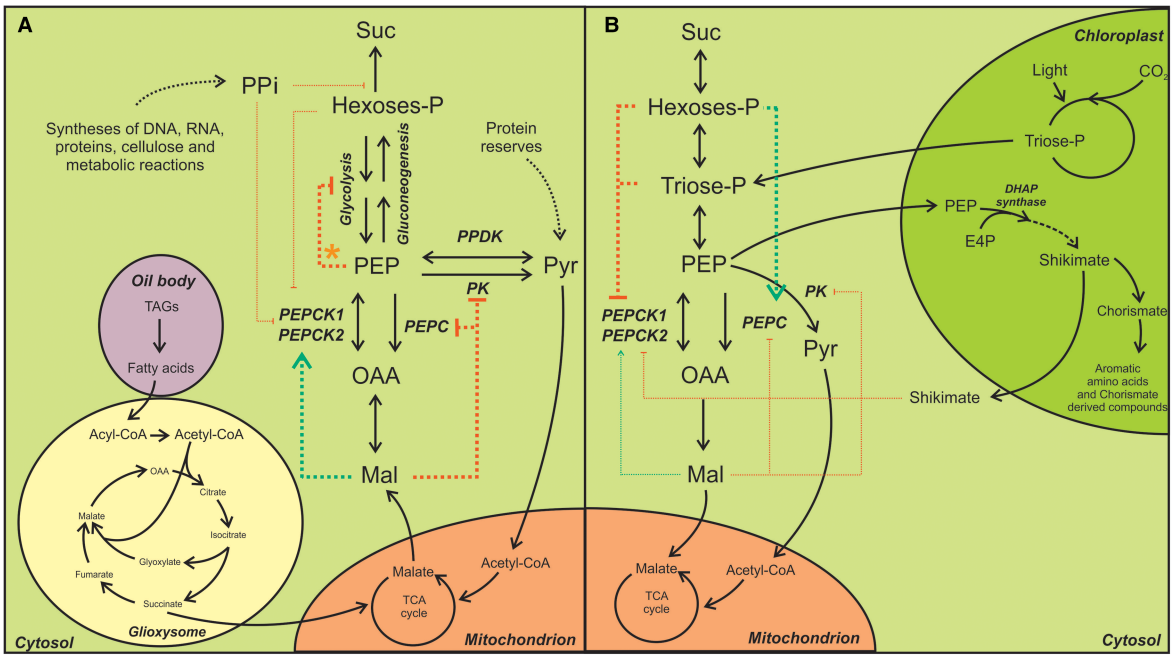

Figure 5. Metabolic model of PEP metabolism in heterotrophic (A) and photoautotrophic (B) tissues.

The enzymes involved in PEP metabolism are PEPCK, phospho*enol*pyruvate carboxykinase (EC 4.1.1.49); PEPC, phospho*enol*pyruvate carboxylase (EC 4.1.1.31); PPDK, pyruvate orthophosphate dikinase (EC 2.7.9.1); PK, pyruvate kinase (EC 2.7.1.40) and DHAP synthase, 3-deoxy-7-phosphoheptunolate synthase (EC 2.5.1.54). * Inhibition of glycolysis by PEP occurs trough inhibition of 6-phosphofructokinase (EC 2.7.1.11) and fructose-bisphosphate aldolase (EC 4.1.2.13) [93–95,38].

A second futile cycle could occur between PEPCK and pyruvate kinase (PK, EC 2.7.1.40), causing the net decarboxylation of OAA to Pyr and CO_2 [1]. In germinating oilseeds two isoenzymes of PK are expressed, one in the plastid and the other one in the cytosol, which accounts for 85% of the total PK activity [71,72]. As with PEPC, malate inhibition of PK [73] would avoid a futile cycle between these enzymes (Figure 5A).

Recently, Ferjani et al. [74] proposed a regulatory role for PPi in gluconeogenesis during seed germination. The role of this metabolite in plant metabolism remained elusive for years [75,76], but these authors reported that knock-out mutants in the vacuolar H^+-translocating pyrophosphatase (*fugu5* mutant) accumulate high levels of PPi in the cytosol, inhibiting the gluconeogenic pathway and arresting the development of Arabidopsis seedlings [75]. The inhibition of gluconeogenesis has been related to product inhibition of UDP-glucose pyrophosphorylase [74], which is strongly inhibited by PPi concentrations lower than 10 mM [77]. As *Ath*PEPCKs are strongly inhibited by PPi (Figure 4 and Table 2), we hypothesize that inhibition of gluconeogenesis might also be the consequence of *Ath*PEPCKs inhibition (Figure 5A).

In other non-photosynthetic tissues, such as fruits, enzymatic control by metabolites could also be of importance. Both malate levels and PEPCK activity peak during tomato and strawberry fruit ripening [26,78–81]. The suppression of the *PEPCK* gene by RNA interference in *Solanoum tuberosum* led to a reduced sugar content accompanied by an increase in malate levels [82,83]. The opposite effect was observed when this gene was over-expressed with the *35S* promoter or with a fruit specific *E8* promoter [84]. Thus, activation of *Ath*PEPCK1 by malate might be a mechanism to channel malate towards gluconeogenesis. Furthermore, the relationship between *Ath*PEPCK1 and malate might be important during stress conditions. Arabidopsis *pepck1* knock-out mutants are more susceptible to drought than wild type plants. Mutant plants are unable to completely close their stomata in the dark [85], which is closely related to malate metabolism [86]. Recently, this relationship has been clearly established as *pepck1* mutants have increased levels of malate, succinate and citrate, and reduced levels of Glc1P, Glc6P and Fru6P [74].

The development of the photosynthetic apparatus leads to a major rearrangement of the metabolic profile of the plant cell [87]. The main carbon source in illuminated leaves comes from trioses-P synthesized by the Benson–Calvin cycle [39,88]. Under this metabolic scenario, there is an exponential increase in the levels of trioses-P and

hexoses-P (Figure 5B). We estimated that the concentrations of hexoses-P in illuminated leaves are within the range of the $I_{0.5}$ values determined for *Ath*PEPCKs (Table 2) [55,87], which are expressed in this tissue [19]. Then, hexoses-P would inhibit PEPCKs and stimulate the activity of PEPC, which is activated by Glc6P [58–64], thus inhibiting gluconeogenesis and stimulating the respiration of the photosynthetically fixed carbon (Figure 5B).

Another function of *Ath*PEPCKs in leaves might be in stress-related metabolic responses. Shikimate metabolism in plants is an intricated network of enzymatic reactions dedicated to the synthesis of the aromatic amino acids (Phe, Trp, Tyr) and a range of metabolic compounds, some of which are related to biotic stress reactions, such as salicylic acid [89]. This pathway takes place mainly in the plastids and starts with the condensation of PEP (derived from glycolysis) with eritrose-4-phosphate (E4P, derived from the pentose phosphate pathway) to form shikimate, the precursor of aromatic amino acids in the plastids and other compounds in the cytosol [89]. Inhibition of *Ath*PEPCK1 by shikimate might be a mechanism to regulate the synthesis of PEP, the initial substrate of the shikimate pathway. It has been described that partitioning of carbon through this pathway is feedback inhibited by the corresponding products of each branch and supply of the initial substrates of the pathway (PEP and E4P) play an important role in the flux through it [89]. The calculated concentration of shikimate in Arabidopsis leaves (1.1 mM) [55,87] is in the range of the $I_{0.5}$ obtained for *Ath*PEPCK1. This relation of *Ath*PEPCKs with the shikimate pathway is reinforced by the fact that in Arabidopsis, the *PEPCK1* gene is strongly induced in leaves upon biotic stress (as it can be seen using data from the gene expression database eFP Browser [90]). Also, mutants in the *PEPCK1* gene show reduced levels of aromatic amino acids in etiolated Arabidopsis seedlings [74] and, in pepper plants where the *PEPCK* gene was silenced the levels of salicylic acid were reduced compared with the *wt* upon bacterial infection [91]. Both aromatic amino acids and salicylic acid represent products of the shikimate pathway [89,92].

The differences found in the regulatory properties of plant PEPCKs (this and further works detailed in Supplementary Table S1) might result from variants in the metabolic pathways operating in diverse plant species. Another possibility is that the kinetic and regulatory properties determined for native PEPCKs purified directly from a plant tissue reflect the response of a mix of phosphorylated (or proteolyzed) and non-phosphorylated enzyme. The development of a system for PEPCK expression and purification will allow us to mimic such modifications by mutagenesis in the near future, to better understand the regulation of this pivotal enzyme.

Abbreviations

3PGA, 3-phosphoglycerate; E4P, erythrose-4-phosphate; Fru6P, fructose 6-phosphate; Fructose 1,6-bisphosphate, Fru1,6bisP; Glc1P, glucose 1-phosphate; Glc6P, glucose 6-phosphate; OAA, oxaloacetic acid; PEP, phospho*enol*pyruvate; PEPC, phosphoenolpyruvate carboxylase; PEPCK, phospho*enol*pyruvate carboxykinase; PK, pyruvate kinase; Pyr, pyruvate.

Author Contributions

F.E.P. and A.A.I. conceived the study. B.E.R., M.D.H. and L.L. performed experiments. B.E.R., M.D.H., C.M.F. and A.A.I. analyzed data and wrote the manuscript. All authors approved the final version of the manuscript.

Funding

This work was supported by grants from ANPCyT (PICT-2015-1767, PICT-2015-1074, PICT-2017-1515), CONICET and UNL (CAI+D 2016, CAI+D Joven 2016).

Acknowledgements

BER is a Fellow from CONICET; CMF, FEP and AAI are Researchers from the same Institution. CMF is funded by the Max Planck Society (Partner Group for Plant Biochemistry).

Competing Interests

The Authors declare that there are no competing interests associated with the manuscript.

References

1 Davies, D.D. (1979) The central role of phosphoenolpyruvate in plant metabolism. *Annu. Rev. Plant Biol.* **30**, 131–158 https://doi.org/10.1146/annurev.pp.30.060179.001023

2 Chiba, Y., Kamikawa, R., Nakada-Tsukui, K., Saito-Nakano, Y. and Nozaki, T. (2015) Discovery of PP_i-type phosphoenolpyruvate carboxykinase genes in Eukaryotes and Bacteria. *J. Biol. Chem.* **290**, 23960–23970 https://doi.org/10.1074/jbc.M115.672907

Biochemical Journal (2019) **476** 2939–2952
https://doi.org/10.1042/BCJ20190523

3 Fukuda, W., Fukui, T., Atomi, H. and Imanaka, T. (2004) First characterization of an archaeal GTP-dependent phosphoenolpyruvate carboxykinase from the hyperthermophilic archaeon *Thermococcus kodakaraensis* KOD1. *J. Bacteriol.* **186**, 4620–4627 https://doi.org/10.1128/JB.186.14.4620-4627.2004

4 Aich, S. and Delbaere, L.T.J. (2007) Phylogenetic study of the evolution of PEP-carboxykinase. *Evol. Bioinform.* **3**, 333–340 https://doi.org/10.1177/117693430700300012

5 Matte, A., Tari, L.W., Goldie, H. and Delbaere, L.T. (1997) Structure and mechanism of phosphoenolpyruvate carboxykinase. *J. Biol. Chem.* **272**, 8105–8108 https://doi.org/10.1074/jbc.272.13.8105

6 Johnson, T.A., McLeod, M.J. and Holyoak, T. (2016) Utilization of substrate intrinsic binding energy for conformational change and catalytic function in phosphoenolpyruvate carboxykinase. *Biochemistry* **55**, 575–587 https://doi.org/10.1021/acs.biochem.5b01215

7 Goldie, A.H. and Sanwal, B.D. (1980) Allosteric control by calcium and mechanism of desensitization of phosphoenolpyruvate carboxykinase of *Escherichia coli*. *J. Biol. Chem.* **255**, 1399–1405 PMID:6986370

8 Burnell, J.N. (1986) Purification and properties of phosphoenolpyruvate carboxykinase from C_4 plants. *Aust. J. Plant Physiol.* **13**, 577–587 https://doi.org/10.1071/pp9860577

9 Edwards, G.E., Kanai, R. and Black, C.C. (1971) Phosphoenolpyruvate carboxykinase in leaves of certain plants which fix CO_2 by the C_4-dicarboxylic acid cycle of photosynthesis. *Biochem. Biophys. Res. Commun.* **45**, 278–285 https://doi.org/10.1016/0006-291X(71)90814-X

10 Reiskind, J.B. and Bowes, G. (1991) The role of phosphoenolpyruvate carboxykinase in a marine macroalga with C4-like photosynthetic characteristics. *Proc. Natl Acad. Sci. U.S.A.* **88**, 2883–2887 https://doi.org/10.1073/pnas.88.7.2883

11 Martín, M., Rius, S.P. and Podestá, F.E. (2011) Two phosphoenolpyruvate carboxykinases coexist in the Crassulacean Acid Metabolism plant *Ananas comosus*. Isolation and characterization of the smaller 65 kDa form. *Plant Physiol. Biochem.* **49**, 646–653 https://doi.org/10.1016/j.plaphy.2011.02.015

12 Leegood, R.C. and Ap Rees, T. (1978) Phosphoenolpyruvate carboxykinase and gluconeogenesis in cotyledons of *Cucurbita pepo*. *Biochim. Biophys. Acta* **524**, 207–218 https://doi.org/10.1016/0005-2744(78)90119-5

13 Trevanion, S.J., Brooks, A.L. and Leegood, R.C. (1995) Control of gluconeogenesis by phospho enolpyruvate carboxykinase in cotyledons of *Cucurbita pepo* L. *Planta* **196**, 653–658 https://doi.org/10.1007/BF01106757

14 Martín, M., Plaxton, W.C. and Podestá, F.E. (2007) Activity and concentration of non-proteolyzed phosphoenolpyruvate carboxykinase in the endosperm of germinating castor oil seeds: effects of anoxia on its activity. *Physiol. Plant.* **130**, 484–494 https://doi.org/10.1111/j.1399-3054.2007.00917.x

15 Eastmond, P.J. and Graham, I.A. (2001) Re-examining the role of the glyoxylate cycle in oilseeds. *Trends Plant Sci.* **6**, 72–78 https://doi.org/10.1016/S1360-1385(00)01835-5

16 Graham, I.A. (2008) Seed storage oil mobilization. *Annu. Rev. Plant Biol.* **59**, 115–142 https://doi.org/10.1146/annurev.arplant.59.032607.092938

17 Walker, R.P., Chen, Z.-H., Técsi, L.I., Famiani, F., Lea, P.J. and Leegood, R.C. (1999) Phosphoenolpyruvate carboxykinase plays a role in interactions of carbon and nitrogen metabolism during grape seed development. *Planta* **210**, 9–18 https://doi.org/10.1007/s004250050648

18 Lea, P.J., Chen, Z.-H., Leegood, R.C. and Walker, R.P. (2001) Does phosphoenolpyruvate carboxykinase have a role in both amino acid and carbohydrate metabolism? *Amino Acids* **20**, 225–241 https://doi.org/10.1007/s007260170041

19 Malone, S., Chen, Z.-H., Bahrami, A.R., Walker, R.P., Gray, J.E. and Leegood, R.C. (2007) Phosphoenolpyruvate carboxykinase in Arabidopsis: changes in gene expression, protein and activity during vegetative and reproductive development. *Plant Cell Physiol.* **48**, 441–450 https://doi.org/10.1093/pcp/pcm014

20 Rylott, E.L., Hooks, M.A. and Graham, I.A. (2001) Co-ordinate regulation of genes involved in storage lipid mobilization in *Arabidopsis thaliana*. *Biochem. Soc. Trans.* **29**, 283–286 https://doi.org/10.1042/bst0290283

21 Rylott, E.L., Gilday, A.D. and Graham, I.A. (2003) The gluconeogenic enzyme phospho*enol*pyruvate carboxykinase in Arabidopsis is essential for seedling establishment. *Plant Physiol.* **131**, 1834–1842 https://doi.org/10.1104/pp.102.019174

22 Penfield, S., Rylott, E.L., Gilday, A.D., Graham, S., Larson, T.R. and Graham, I.A. (2004) Reserve mobilization in the Arabidopsis endosperm fuels hypocotyl elongation in the dark, is independent of abscisic acid, and requires *PHOSPHOENOLPYRUVATE CARBOXYKINASE1*. *Plant Cell* **16**, 2705–2718 https://doi.org/10.1105/tpc.104.024711

23 Eastmond, P.J., Astley, H.M., Parsley, K., Aubry, S., Williams, B.P., Menard, G.N. et al. (2015) Arabidopsis uses two gluconeogenic gateways for organic acids to fuel seedling establishment. *Nat. Commun.* **6**, 6659 https://doi.org/10.1038/ncomms7659

24 Huala, E., Dickerman, A.W., Garcia-Hernandez, M., Weems, D., Reiser, L., LaFond, F., et al. (2001) The Arabidopsis Information Resource (TAIR): a comprehensive database and web-based information retrieval, analysis, and visualization system for a model plant. *Nucleic Acids Res.* **29**, 102–105 https://doi.org/10.1093/nar/29.1.102

25 Ericsson, U.B., Hallberg, B.M., DeTitta, G.T., Dekker, N. and Nordlund, P. (2006) Thermofluor-based high-throughput stability optimization of proteins for structural studies. *Anal. Biochem.* **357**, 289–298 https://doi.org/10.1016/j.ab.2006.07.027

26 Ruffner, H.P. and Kliewer, W.M. (1975) Phosphoenolpyruvate carboxykinase activity in grape berries. *Plant Physiol.* **56**, 67–71 https://doi.org/10.1104/pp.56.1.67

27 Ray, T.B. and Black, C.C. (1976) Characterization of phosphoenolpyruvate carboxykinase from *Panicum maximum*. *Plant Physiol.* **58**, 603–607 https://doi.org/10.1104/pp.58.5.603

28 Daley, L.S., Ray, T.B., Vines, H.M. and Black, C.C. (1977) Characterization of phosphoenolpyruvate carboxykinase from pineapple leaves *Ananas comosus* (L.) Merr. *Plant Physiol.* **59**, 618–622 https://doi.org/10.1104/pp.59.4.618

29 Walker, R.P. and Leegood, R.C. (1995) Purification, and phosphorylation in vivo and in vitro, of phospho*enol*pyruvate carboxykinase from cucumber cotyledons. *FEBS Lett.* **362**, 70–74 https://doi.org/10.1016/0014-5793(95)00212-R

30 Ferreira, C.M.H., Pinto, I.S.S., Soares, E.V. and Soares, H.M.V.M. (2015) (Un)suitability of the use of pH buffers in biological, biochemical and environmental studies and their interaction with metal ions – a review. *RSC Adv.* **5**, 30989–31003 https://doi.org/10.1039/C4RA15453C

31 Raven, J.A. (1985) Ph regulation in plants. *Sci. Progess* **69**, 495–509 https://www.jstor.org/stable/43420618

32 Davies, D.D. (1986) The fine control of cytosolic pH. *Physiol. Plant.* **67**, 702–706 https://doi.org/10.1111/j.1399-3054.1986.tb05081.x

33 Shen, J., Zeng, Y., Zhuang, X., Sun, L., Yao, X., Pimpl, P. et al. (2013) Organelle pH in the Arabidopsis endomembrane system. *Mol. Plant* **6**, 1419–1437 https://doi.org/10.1093/mp/sst079

34 Gupta, R.K., Oesterling, R.M. and Mildvan, A.S. (1976) Dual divalent cation requirement for activation of pyruvate kinase: essential roles of both enzyme- and nucleotide-bound metal ions. *Biochemistry* **15**, 2881–2887 https://doi.org/10.1021/bi00658a028

35 Quiquampoix, H., Loughman, B.C. and Ratcliffe, R.G. (1993) A ^{31}P-NMR study of the uptake and compartmentation of manganese by maize roots. *J. Exp. Bot.* **44**, 1819–1827 https://doi.org/10.1093/jxb/44.12.1819
36 Pittman, J.K. and Pittman, J.K. (2005) Managing the manganese : molecular mechanisms of manganese transport and homeostasis. *New Phytol.* **167**, 733–742 https://doi.org/10.1111/j.1469-8137.2005.01453.x
37 Chen, Z.-H., Walker, R.P., Acheson, R.M. and Leegood, R.C. (2002) Phospho*enol*pyruvate carboxykinase assayed at physiological concentrations of metal ions has a high affinity for CO_2. *Plant Physiol.* **128**, 160–164 https://doi.org/10.1104/pp.010431
38 Plaxton, W.C. (1996) The organization and regulation of plant glycolysis. *Annu. Rev. Plant Physiol. Plant Mol. Biol.* **47**, 185–214 https://doi.org/10.1146/annurev.arplant.47.1.185
39 Plaxton, W.C. and Podestá, F.E. (2006) The functional organization and control of plant respiration. *Crit. Rev. Plant Sci.* **25**, 159–198 https://doi.org/10.1080/07352680600563876
40 Nielsen, T.H., Rung, J.H. and Villadsen, D. (2004) Fructose-2,6-biphosphatase: a traffic signal in plant metabolism. *Trends Plant Sci.* **9**, 556–563 https://doi.org/10.1016/j.tplants.2004.09.004
41 Veyel, D., Sokolowska, E.M., Moreno, J.C., Kierszniowska, S., Cichon, J., Wojciechowska, I., et al. (2018) PROMIS, global analysis of PROtein–metabolite interactions using size separation in *Arabidopsis thaliana*. *J. Biol. Chem.* **293**, 12440–12453 https://doi.org/10.1074/jbc.RA118.003351
42 Lo, M.-C., Aulabaugh, A., Jin, G., Cowling, R., Bard, J., Malamas, M. et al. (2004) Evaluation of fluorescence-based thermal shift assays for hit identification in drug discovery. *Anal. Biochem.* **332**, 153–159 https://doi.org/10.1016/j.ab.2004.04.031
43 Niesen, F.H., Berglund, H. and Vedadi, M. (2007) The use of differential scanning fluorimetry to detect ligand interactions that promote protein stability. *Nat. Protoc.* **2**, 2212–2221 https://doi.org/10.1038/nprot.2007.321
44 Fedorov, O., Niesen, F.H. and Knapp, S. (2012) Kinase inhibitor selectivity profiling using differential scanning fluorimetry BT - kinase inhibitors: methods and protocols. *Methods Mol. Biol.* **795**, 109–118 https://doi.org/10.1007/978-1-61779-337-0_7
45 Rudolf, A.F., Skovgaard, T., Knapp, S., Jensen, L.J. and Berthelsen, J. (2014) A comparison of protein kinases inhibitor screening methods using both enzymatic activity and binding affinity determination. *PLoS One* **9**, e98800 https://doi.org/10.1371/journal.pone.0098800
46 Leegood, R.C. and Walker, R.P. (1996) Phosphorylation of phosphoenolpyruvate carboxykinase in plants. Studies in plants with C_4 photosynthesis and Crassulacean acid metabolism and in germinating seeds. *Biochem. J.* **317**, 653–658 https://doi.org/10.1042/bj3170653
47 Piattoni, C.V., Rius, S.P., Gomez-Casati, D.F., Guerrero, S.A. and Iglesias, A.A. (2010) Heterologous expression of non-phosphorylating glyceraldehyde-3-phosphate dehydrogenase from *Triticum aestivum* and *Arabidopsis thaliana*. *Biochimie* **92**, 909–913 https://doi.org/10.1016/j.biochi.2010.03.017
48 Hartman, M.D., Figueroa, C.M., Arias, D.G. and Iglesias, A.A. (2016) Inhibition of recombinant aldose-6-phosphate reductase from peach leaves by hexose-phosphates, inorganic phosphate and oxidants. *Plant Cell Physiol.* **58**, 145–155 https://doi.org/10.1093/pcp/pcw180
49 Arnelle, D.R. and O'leary, M.H. (1992) Binding of carbon dioxide to phosphoenolpyruvate carboxykinase deduced from carbon kinetic isotope effects. *Biochemistry* **31**, 4363–4368 https://doi.org/10.1021/bi00132a029
50 Walker, R.P., Trevanion, S.J. and Leegood, R.C. (1995) Phosphoenolpyruvate carboxykinase from higher plants: purification from cucumber and evidence of rapid proteolytic cleavage in extracts from a range of plant tissues. *Planta* **196**, 58–63 https://doi.org/10.1007/BF00193217
51 Latorre-Muro, P., Baeza, J., Armstrong, E.A., Hurtado-Guerrero, R., Corzana, F., Wu, L.E. et al. (2018) Dynamic acetylation of phosphoenolpyruvate carboxykinase toggles enzyme activity between gluconeogenic and anaplerotic reactions. *Mol. Cell* **71**, 718–732.e9 https://doi.org/10.1016/j.molcel.2018.07.031
52 Pantoliano, M.W., Petrella, E.C., Kwasnoski, J.D., Lobanov, V.S., Myslik, J., Graf, E., et al. (2001) High-density miniaturized thermal shift assays as a general strategy for drug discovery. *J. Biomol. Screen.* **6**, 429–440 https://doi.org/10.1177/108705710100600609
53 Hatch, M.D. and Mau, S. (1977) Properties of phosphoenolpyruvate carboxykinase operative in C_4 pathway photosynthesis. *Funct. Plant Biol.* **4**, 207–216 https://doi.org/10.1071/PP9770207
54 Kim, D.-J. and Smith, S.M. (1994) Molecular cloning of cucumber phosphoenolpyruvate carboxykinase and developmental regulation of gene expression. *Plant Mol. Biol.* **26**, 423–434 https://doi.org/10.1007/BF00039551
55 Koffler, B.E., Bloem, E., Zellnig, G. and Zechmann, B. (2013) High resolution imaging of subcellular glutathione concentrations by quantitative immunoelectron microscopy in different leaf areas of Arabidopsis. *Micron* **45**, 119–128 https://doi.org/10.1016/j.micron.2012.11.006
56 Fait, A., Angelovici, R., Less, H., Ohad, I., Urbanczyk-Wochniak, E., Fernie, A.R. et al. (2006) Arabidopsis seed development and germination is associated with temporally distinct metabolic switches. *Plant Physiol.* **142**, 839–854 https://doi.org/10.1104/pp.106.086694
57 Presiss, J. and Kosuge, T. (1976) Regulation of enzyme activity in metabolic pathways. In *Plant Biochemistry* (Bonner, J. and Varner, J. E. B. T.-P. B., eds.), pp. 277–336, Academic Press, San Diego
58 Gonzalez, D.H., Iglesias, A.A. and Andreo, C.S. (1984) On the regulation of phosphoenolpyruvate carboxylase activity from maize leaves by L-malate. Effect of pH. *J. Plant Physiol.* **116**, 425–434 https://doi.org/10.1016/S0176-1617(84)80134-0
59 Andreo, C.S., Gonzalez, D.H. and Iglesias, A.A. (1987) Higher plant phospho*enol*pyruvate carboxylase. Structure and regulation. *FEBS Lett.* **213**, 1–8 https://doi.org/10.1016/0014-5793(87)81454-0
60 McNaughton, G.A., Fewson, C.A., Wilkins, M.B. and Nimmo, H.G. (1989) Purification, oligomerization state and malate sensitivity of maize leaf phosphoenolpyruvate carboxylase. *Biochem. J.* **261**, 349–355 https://doi.org/10.1042/bj2610349
61 Wedding, R.T., Black, M.K. and Meyer, C.R. (1990) Inhibition of phospho*enol*pyruvate carboxylase by malate. *Plant Physiol.* **92**, 456–461 https://doi.org/10.1104/pp.92.2.456
62 Bakrim, N., Nhiri, M., Pierre, J.-N. and Vidal, J. (1998) Metabolite control of Sorghum C4 phosphoenolpyruvate carboxylase catalytic activity and phosphorylation state. *Photosynth. Res.* **58**, 153–162 https://doi.org/10.1023/A:1006164209129
63 Nhiri, M., Bakrim, N., Bakrim, N., El Hachimi-Messouak, Z., Echevarria, C. and Vidal, J. (2000) Posttranslational regulation of phosphoenolpyruvate carboxylase during germination of Sorghum seeds: influence of NaCl and L-malate. *Plant Sci.* **151**, 29–37 https://doi.org/10.1016/S0168-9452(99)00191-0
64 Feria, A.-B., Alvarez, R., Cochereau, L., Vidal, J., García-Maurino, S. and Echevarria, C. (2008) Regulation of phospho*enol*pyruvate carboxylase phosphorylation by metabolites and abscisic acid during the development and germination of barley seeds. *Plant Physiol.* **148**, 761–774 https://doi.org/10.1104/pp.108.124982
65 Walker, R.P., Acheson, R.M., Tecsi, L.I. and Leegood, R.C. (1997) Phosphoenolpyruvate carboxykinase in C4 plants: its role and regulation. *Aust. J. Plant Physiol.* **24**, 459–468 https://doi.org/10.1071/pp97007

Biochemical Journal (2019) **476** 2939–2952
https://doi.org/10.1042/BCJ20190523

66 Walker, R.P., Chen, Z.-H., Acheson, R.M. and Leegood, R.C. (2002) Effects of phosphorylation on phospho*enol*pyruvate carboxykinase from the C 4 plant Guinea grass. *Plant Physiol.* **128**, 165–172 https://doi.org/10.1104/pp.010432
67 Leegood, R.C. and Walker, R.P. (2003) Regulation and roles of phosphoenolpyruvate carboxykinase in plants. *Arch. Biochem. Biophys.* **414**, 204–210 https://doi.org/10.1016/S0003-9861(03)00093-6
68 Chao, Q., Liu, X.-Y., Mei, Y.-C., Gao, Z.-F., Chen, Y.-B., Qian, C.-R. et al. (2014) Light-regulated phosphorylation of maize phosphoenolpyruvate carboxykinase plays a vital role in its activity. *Plant Mol. Biol.* **85**, 95–105 https://doi.org/10.1007/s11103-014-0171-3
69 Bailey, K.J., Gray, J.E., Walker, R.P. and Leegood, R.C. (2007) Coordinate regulation of phospho*enol*pyruvate carboxylase and phospho*enol*pyruvate carboxykinase by light and CO_2 during C_4 photosynthesis. *Plant Physiol.* **144**, 479–486 https://doi.org/10.1104/pp.106.093013
70 Durek, P., Schmidt, R., Heazlewood, J.L., Jones, A., MacLean, D., Nagel, A. et al. (2010) Phosphat: the *Arabidopsis thaliana* phosphorylation site database. An update. *Nucleic Acids Res.* **38**, D828–D834 https://doi.org/10.1093/nar/gkp810
71 Plaxton, W.C. (1988) Purification of pyruvate kinase from germinating castor bean endosperm. *Plant Physiol.* **86**, 1064–1069 https://doi.org/10.1104/pp.86.4.1064
72 Plaxton, W.C. (1989) Molecular and immunological characterization of plastid and cytosolic pyruvate kinase isozymes from castor-oil-plant endosperm and leaf. *Eur. J. Biochem.* **181**, 443–451 https://doi.org/10.1111/j.1432-1033.1989.tb14745.x
73 Podesta, F.E. and Plaxton, W.C. (1991) Kinetic and regulatory properties of cytosolic pyruvate kinase from germinating castor oil seeds. *Biochem J.* **279**, 495–501 https://doi.org/10.1042/bj2790495
74 Ferjani, A., Kawade, K., Asaoka, M., Oikawa, A., Okada, T., Mochizuki, A. et al. (2018) Pyrophosphate inhibits gluconeogenesis by restricting UDP-glucose formation in vivo. *Sci. Rep.* **8**, 1–10 https://doi.org/10.1038/s41598-018-32894-1
75 Ferjani, A., Segami, S., Horiguchi, G., Muto, Y., Maeshima, M. and Tsukaya, H. (2011) Keep an eye on PPi : the vacuolar-type H^+-pyrophosphatase regulates postgerminative development in Arabidopsis. *Plant Cell* **23**, 2895–2908 https://doi.org/10.1105/tpc.111.085415
76 Heinonem, J.K. (2001) *Biological Role of Inorganic Phosphate*, Springer Science+Businness Media, LLC, New York
77 Okazaki, Y., Shimojima, M., Sawada, Y., Toyooka, K., Narisawa, T., Mochida, K., et al. (2009) A chloroplastic UDP-glucose pyrophosphorylase from Arabidopsis is the committed enzyme for the first step of sulfolipid biosynthesis. *Plant Cell* **21**, 892–909 https://doi.org/10.1105/tpc.108.063925
78 Famiani, F., Farinelli, D., Palliotti, A., Moscatello, S., Battistelli, A. and Walker, R.P. (2014) Is stored malate the quantitatively most important substrate utilised by respiration and ethanolic fermentation in grape berry pericarp during ripening ? *Plant Physiol. Biochem.* **76**, 52–57 https://doi.org/10.1016/j.plaphy.2013.12.017
79 Sweetman, C., Deluc, L.G., Cramer, G.R., Ford, C.M. and Soole, K.L. (2009) Regulation of malate metabolism in grape berry and other developing fruits. *Phytochemistry* **70**, 1329–1344 https://doi.org/10.1016/j.phytochem.2009.08.006
80 Walker, R.P., Paoletti, A., Leegood, R.C. and F, F. (2016) Phosphorylation of phosphoenolpyruvate carboxykinase (PEPCK) and phosphoenolpyruvate carboxylase (PEPC) in the flesh of fruits. *Plant Physiol. Biochem.* **108**, 323–327 https://doi.org/10.1016/j.plaphy.2016.07.021
81 Famiani, F., Farinelli, D., Moscatello, S., Battistelli, A., Leegood, R.C. and Walker, R.P. (2016) The contribution of stored malate and citrate to the substrate requirements of metabolism of ripening peach (*Prunus persica* L. Batsch) flesh is negligible. Implications for the occurrence of phosphoenolpyruvate carboxykinase and gluconeogenesis. *Plant Physiol. Biochem.* **101**, 33–42 https://doi.org/10.1016/j.plaphy.2016.01.007
82 Huang, Y.-X., Yin, Y.-G., Sanuki, A., Fukuda, N., Ezura, H. and Matsukura, C. (2015) Phosphoenolpyruvate carboxykinase (PEPCK) deficiency affects the germination, growth and fruit sugar content in tomato (*Solanum lycopersicum* L.). *Plant Physiol. Biochem.* **96**, 417–425 https://doi.org/10.1016/j.plaphy.2015.08.021
83 Osorio, S., Vallarino, J.G., Szecowka, M., Ufaz, S., Tzin, V., Angelovici, R. et al. (2013) Alteration of the interconversion of pyruvate and malate in the plastid or cytosol of ripening tomato fruit invokes diverse consequences on sugar but similar effects on cellular organic acid, metabolism, and transitory starch accumulation. *Plant Physiol.* **161**, 628–643 https://doi.org/10.1104/pp.112.211094
84 Huang, Y.-X., Goto, Y., Nonaka, S., Fukuda, N., Ezura, H. and Matsukura, C. (2015) Overexpression of the phosphoenolpyruvate carboxykinase gene (SlPEPCK) promotes soluble sugar accumulation in fruit and post-germination growth of tomato (*Solanum lycopersicum* L.). *Plant Biotechnol.* **32**, 281–289 https://doi.org/10.5511/plantbiotechnology.15.1019a
85 Penfield, S., Clements, S., Bailey, K.J., Gilday, A.D., Leegood, R.C., Gray, J.E. et al. (2012) Expression and manipulation of PHOSPHOENOLPYRUVATE CARBOXYKINASE 1 identifies a role for malate metabolism in stomatal closure. *Plant J.* **69**, 679–688 https://doi.org/10.1111/j.1365-313X.2011.04822.x
86 Azoulay-Shemer, T., Bagheri, A., Wang, C., Palomares, A., Stephan, A.B., Kunz, H.-H. et al. (2016) Starch biosynthesis in guard cells but not in mesophyll cells is involved in CO2-induced stomatal closing. *Plant Physiol.* **171**, 788–798 https://doi.org/10.1104/pp.15.01662
87 Szecowka, M., Heise, R., Tohge, T., Nunes-Nesi, A., Vosloh, D., Huege, J., et al. (2013) Metabolic fluxes in an illuminated Arabidopsis rosette. *Plant Cell* **25**, 694–714 https://doi.org/10.1105/tpc.112.106989
88 Iglesias, A. A. and Podestá, F. E. (2005) Photosynthate formation and partitionning in crop plants. In *Handbook of Photosynthesis* (Pessarakli, M., ed.), pp. 525–546, CRC Press, Boca Raton
89 Maeda, H. and Dudareva, N. (2012) The shikimate pathway and aromatic amino acid biosynthesis in plants. *Annu. Rev. Plant Biol.* **63**, 73–105 https://doi.org/10.1146/annurev-arplant-042811-105439
90 Winter, D., Vinegar, B., Nahal, H., Ammar, R., Wilson, G.V. and Provart, N.J. (2007) An "Electronic Fluorescent Pictograph" browser for exploring and analyzing large-scale biological data sets. *PLoS One* **2**, e718 https://doi.org/10.1371/journal.pone.0000718
91 Choi, D.S., Kim, N.H. and Hwang, B.K. (2015) The pepper phosphoenolpyruvate carboxykinase CaPEPCK1 is involved in plant immunity against bacterial and oomycete pathogens. *Plant Mol. Biol.* **89**, 99–111 https://doi.org/10.1007/s11103-015-0354-6
92 Dempsey, D.A., Vlot, A.C., Wildermuth, M.C. and Klessig, D.F. (2011) Salicylic acid biosynthesis and metabolism. *Arabidopsis Book* **9**, e0156 https://doi.org/10.1199/tab.0156
93 Häusler, R.E., Holtum, J.A. and Latzko, E. (1989) Cytosolic phosphofructokinase from spinach leaves : I. Purification, characteristics, and regulation. *Plant Physiol.* **90**, 1498–1505 https://doi.org/10.1104/pp.90.4.1498
94 Moorhead, G.B.G. and Plaxton, W.C. (1990) Purification and characterization of cytosolic aldolase from carrot storage root. *Biochem. J.* **269**, 133–139 https://doi.org/10.1042/bj2690133
95 Botha, F.C. and O'Kennedy, M.M. (1989) Characterization of the cytosolic aldolase from germinating *Phaseolus vulgaris* seeds. *J. Plant Physiol.* **135**, 433–438 https://doi.org/10.1016/S0176-1617(89)80100-2